Journal of Engineering Physics and Thermophysics, Vol. 79, No. 5, 2006

CARRYING BODIES WITH AN ADVERSE LONGITUDINAL PRESSURE GRADIENT

I. I. Mazhul' and R. D. Rakhimov

UDC 533.601.155

Features of formation of an adverse longitudinal pressure gradient in a supersonic flow around a carrying body with a surface inclined at a constant angle to its symmetry plane have been numerically investigated within the framework of the Euler equations. A mathematical model of such bodies constructed on the basis of pieces cut from the surface of a backward-facing hyperelliptic cone is proposed. This model allows one to obtain a wide variety of carrying bodies. The data obtained were compared with the corresponding data for equivalent bodies with a plane downstream face.

Introduction. To increase the efficiency of a hypersonic flying vehicle with an air-breathing engine it is necessary to improve its aerodynamic form. The total aerodynamic thrust characteristics of such a vehicle are determined to a large extent by the integration of its air intake with the glider. The air path of the propulsion system of flying vehicles is usually located under their downstream face. Therefore, the efficiency of the air intake and, consequently, of the vehicle as a whole will depend on the precompression of an air flow by the nose of this vehicle.

Hypersonic flying vehicles with a nose having a plane or a transverse-convex downstream face are the most popular. In an air flow around such a body there usually arises a compression shock separating from its leading edge, which leads to the side spreading of the flow and, as a consequence, to a decrease in the compression. An alternative to these vehicles may be the so-called waveplanes that are constructed using gas-dynamics methods by the lines of known flows. Waveplanes are constructed such that in an air flow around them there arises a compression shock attaching to their leading edges, which completely excludes the side spreading of the flow and makes it possible to easily estimate the characteristics of the flow upstream of the air intake. For example, waveplanes constructed on the basis of a two-dimensional flow downstream of an oblique compression shock are relatively simply integrated with plane air intakes.

Along with plane air intakes, three-dimensional air intakes hold much promise. In this respect, of great interest are air intakes of a new class — the so-called convergent air intakes [1, 2], in which an air flow is compressed along the convergent streamlines. Such air intakes provide a larger degree of compression of an air flow than the plane air intakes and have an inner channel with a more compact cross section, which makes the provision of the heat shield of the walls of hypersonic jet engines much easier. However, their integration on a flying vehicle calls for the development of new forms of precompression surfaces. For example, sector or chute convergent air intakes [2] have an arched concave leading edge, to which the nose part of a vehicle should correspond.

For the purpose of investigating the above-indicated features of the integration of three-dimensional convergent air intakes, bodies with a transverse-concave downstream face representing a piece cut from the surface of a backward-facing axisymmetric circular cone were considered in [3, 4]. Such surfaces have two advantages. First, they are integrated simply with chute convergent air intakes. Second, as calculations have shown [3, 4], a positive pressure gradient arises along such a surface and, therefore, a flow in the end cross section of a vehicle is compressed to a larger extent as compared to that provided by a plane surface.

The use of transverse-concave surfaces in combination with a chute convergent air intake had made it possible to realize a convergent compression of the whole jet entrained by the air intake [5]. In [4], the possibility of increasing the above-indicated adverse longitudinal pressure gradient by rounding of the nose part of a vehicle was consid-

Institute of Theoretical and Applied Mechanics, Siberian Branch of the Russian Academy of Sciences, 4/1 Institutskaya Str., Novosibirsk, 630090, Russia; email: mazhul@itam.nsc.ru. Translated from Inzhenerno-Fizicheskii Zhurnal, Vol. 79, No. 5, pp. 100–108, September–October, 2006. Original article submitted January 28, 2005; revision submitted April 12, 2005.

1062-0125/06/7905-0943

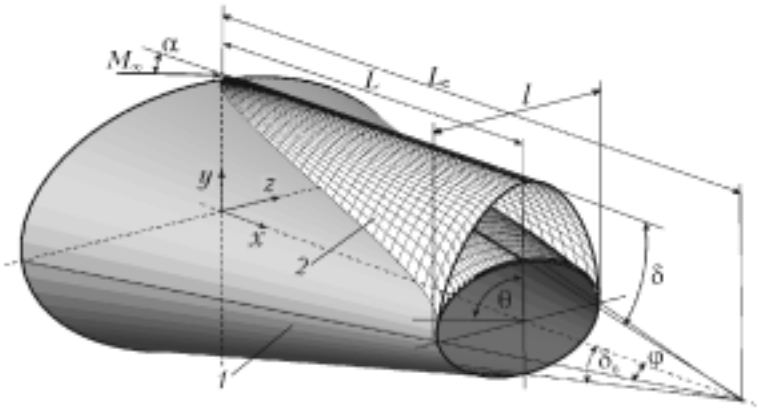

Fig. 1. Scheme of construction and general form of a configuration: 1) backward-facing hyperelliptic cone; 2) body.

ered. However, this method was found to be inefficient because, even though the flow around the nose part of such a body was two-dimensional, the pressure downstream of it decreased and the pressure at the end cross section of the body did not exceed the analogous pressure of a pointed body.

The aim of the present work was to find new aerodynamic forms providing an increase in the compression of the flow at the end cross section of a flying vehicle without an additional longitudinal bending of its surface. We propose a more general approach to the construction of carrying bodies with a transverse-concave downstream face, which includes the method of [3, 4] as a particular case. The form of a flying body in plan was described with the use of power functions, which allowed us to obtain a rounded nose part and leading edges with a variable sweep along their length. As an initial forming body, we used a backward-facing hyperelliptic cone, which made it possible to construct flying bodies with downstream faces of various curvature and shape and, therefore, to investigate the possibility of obtaining a longitudinal compression of an air flow and increasing the pressure at the end cross section of a body, i.e., at the site of location of an air intake, in more detail.

Mathematical Model of a Carrying Body. We will consider three-dimensional carrying bodies, whose compression surface represents a piece cut from the surface of a backward-facing hyperelliptic cone. The scheme of construction of such a body and its general form as well as the coordinate system and designations being used are shown in Fig. 1.

In numerical calculations, we will use a mathematical model describing the form of the indicated bodies in plan with the use of power functions. The cross sections of a body will be defined using the equation of a cone with a hyperelliptic cross section. Thus, the form of a body in plan, determining the transverse coordinates of its leading edge, is defined as

$$z_{\text{pl}} = Ax^n, \tag{1}$$

where A is a constant coefficient. If the length of the body L is known, all integral characteristics of its form in plan can be determined from relation (1). Hereinafter we will consider a class of bodies with a constant length L and a constant elongation λ. In this case, the coefficient $A = \lambda/[2(n+1)L^{n-1}]$ and the form of a body in plan in the coordinates normalized to its length will be defined as

$$\bar{z}_{\text{pl}} = \frac{\lambda}{2(n+1)}\bar{x}^n, \tag{2}$$

where $0 \le \bar{x} = x/L \le 1$.

Bodies with differents forms in plan can be obtained by varying the exponent n. A "classical" triangular configuration is obtained at $n = 1$, a pointed configuration with a concave longitudinal profile is obtained at $n > 1$, and a rounded configuration with a convex longitudinal profile of the leading edges is obtained at $n < 1$. For the given in-

vestigation, of most interest are bodies with $n \le 1$, i.e., bodies having a triangular form in plan or bodies with a rounded nose part. The last-mentioned bodies have leading edges with a sweep varying along their length.

The downstream face of the bodies being considered will be described by the equation of a hyperellipse, which, in the cross section x = const, has the form

$$\frac{z^k}{a_x^k} + \frac{y^k}{b_x^k} = 1 , \tag{3}$$

where $a_x = (L_c - x) \tan \varphi$ and $b_x = (L_c - x) \tan \delta_c$. Relation (3) can be used for a wide variety of cross sections — from a round cross section to a rectangular one. For example, we will obtain a circle at $k = 2$ and $a_x = b_x$, an ellipse at $k = 2$ and $a_x > b_x$, and a near-rectangle cross section at $k \to \infty$.

In view of relation (3), the equation for the downstream face of a body at x = const can be written in coordinates normalized to the length of the body as

$$\bar{y} = \left[(\bar{L}_c - \bar{x})^k \tan^k \delta_c - \lambda_c^k \bar{z}^k \right]^{1/k} , \tag{4}$$

where $0 \le \bar{z} \le \bar{z}_{pl}$. The downstream face constructed in this way has a transverse curvature increasing along the length of the body. In this case, the angle of inclination of the surface of the body to its symmetry plane remains constant and is equal to the forming-cone angle, i.e., $\delta = \delta_c$ = const.

The length of the hyperelliptic cone appearing in relations (3) and (4) can be an independent variable; however, it is more informative to use, as an independent parameter, the angle of opening θ of the leading edges at the end cross section of the body $x = L$. In this case, we obtain that

$$\bar{L}_c = 1 + \frac{\lambda}{2\,(n+1)} \frac{(\lambda_c^k \sin^k \theta + \cos^k \theta)^{1/k}}{\tan \delta_c \sin \theta} .$$

The coordinates of the leading edges of the body are determined from Eqs. (2) and (4) at $\bar{z} = \bar{z}_{pl}$. It should be noted that the edges of the bodies being considered represent curvilinear spatial lines even in the case where these bodies have a triangular form in plan.

The upstream face of a body is constructed by moving the generating line along its leading edges parallel to the axis of the hyperelliptic cone. When the angle of attack is equal to zero, it is parallel to the velocity vector of the incident flow. Its curvature in the transverse direction depends on the form of the body in plan and the transverse profile of the downstream face.

Thus, the surface of the bodies being considered can be defined by the independent quantities n, λ, L, k, δ, φ, and θ, the first three of which determine their form in plan the others determining the form of the cross section. Varying these parameters, we can obtain a large variety of bodies necessary for the problem being solved. For example, configurations with a pointed or a rounded form in plan and a downstream face representing a piece cut from the surface of a backward-facing circular, elliptic, or hyperelliptic cone can be constructed.

The possible advantages of the bodies being considered were determined by comparison of these bodies with bodies equivalent to them with a plane downstream face. Equivalent bodies of both classes have equal lengths, identical forms in plan, and equal thicknesses in the symmetry plane. These conditions are fulfilled at constant values of the parameters n, λ, L, and δ.

Method and Conditions of Calculations. A supersonic, three-dimensional, nonviscous steady flow around the carrying bodies being considered was investigated with the use of the algorithm for numerical solution of Euler equations, described in detail in [6, 7]. We used the marching approach because a purely supersonic flow arises at definite parameters of an incident flow. The integration along the marching direction was performed using explicit Runge–Kutta TVD schemes of high orders of approximation (as high as the third order) [8], providing a monotone solution and a through calculation of flows with gasdynamic separations without introduction of an artificial viscosity. The flows at the faces between the computational cells were determined from the solution of the problem on the interaction

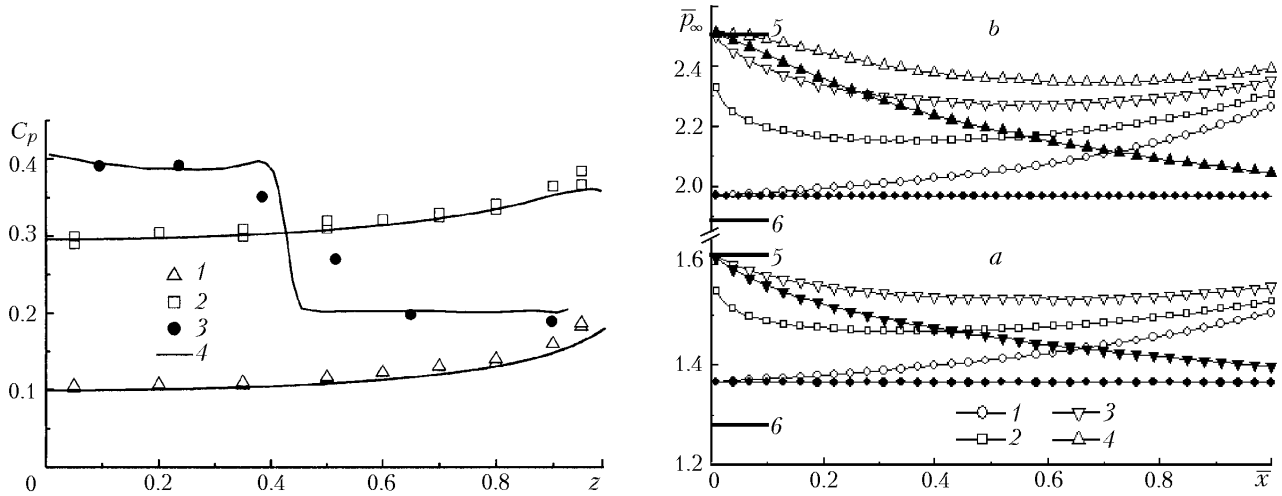

Fig. 2. Comparison of calculation and experimental data: 1) delta-like wing at $\alpha = -0.9^o$; 2) delta-like wing at $\alpha = 9.3^o$; 3) V-like wing at $\alpha = 8.2^o$; 4) numerical calculation.

Fig. 3. Dependence of the pressure distribution along the length of a body in the symmetry plane on its form in plan ($\delta = 5^o$ (a) and 10^o (b)): n = 1 (1), 0.7 (2), 0.5 (3), and 0.4 (4); 5) wedge; 6) cone; filled points are equivalent bodies.

of supersonic flows by the Godunov iteration method [9]. The parameters of the flow at the faces of a cell were determined by averaging their values in the volume of the cell with the use of the van Leer MUSCL method of the third order of approximation [10].

A computational grid was constructed using the multiblock approach. The computational region in each cross section of a body was divided into three zones with a common point at the leading edge of the body. The nodes at the boundaries between the neighboring zones were common, and nodes inside different zones of the grid were generated completely independently. The number of grid nodes in each computational cross section was equal to 200 × 200, and the number of steps in the marching direction was about $(10–12)\cdot 10^3$ when integration was performed to the end cross section.

For verification of the numerical algorithm being used, we calculated three-dimensional configurations close in form to the bodies being considered and compared the data obtained with experimental data. Bodies with a plane downstream face and a triangular cross section (delta-like wings with $\delta = 10.9^o$ and $\lambda = 1.33$) [11] and bodies with a transverse-concave profile (V-like wings with $\delta = 10^o$, $\lambda = 3.1$, and a calculated Mach number of 2.5) [12] were investigated. The results of comparison of the data obtained for these bodies at $M_\infty = 4$ are presented in Fig. 2. It is seen that the calculation and experimental data obtained for the delta-like wings and for the regions of the V-like wings located outside the flow-separation region are in good agreement. In the last-mentioned case, the separation regions arise as a result of the interaction of the internal compression shock with the boundary layer. The calculation data obtained at a later time show that distributed pressure gradients or internal compression shocks, capable of inducing separations of the turbulent boundary layer, do not arise on the bodies being considered. It should be noted that calculations of an ideal-gas flow around these bodies allow one to investigate them in more detail and determine the "critical" regimes of flow around the indicated bodies; these regimes can be verified with the use of viscous models.

The main calculations were performed for an incident flow with a Mach number $M_\infty = 4$ and a zero angle of attack; however, some data were obtained for $M_\infty = 8$. We considered configurations of constant elongation $\lambda = 0.7$ and length L.

Analysis and Results. Let first analyze the numerical data obtained for the simplest case, namely, for a body having a triangular form in plan with a downstream face representing a piece cut from the surface of a backward-facing axisymmetric cone. Such a configuration has the following parameters: $\delta_c = \varphi$, $k = 2$, $n = 1$. Figure 3 presents an example of determining the relative pressure $\bar{p}$ along the length of the indicated body in its symmetry plane at a Mach

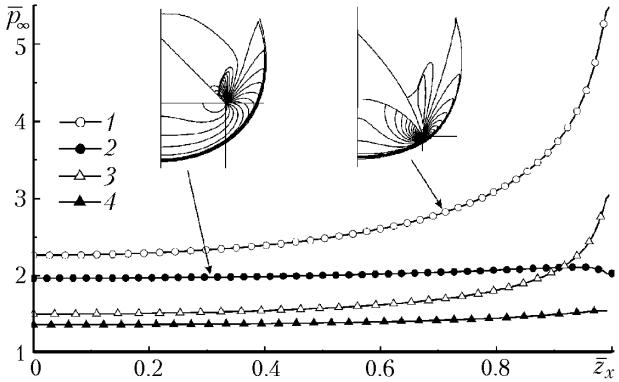

Fig. 4. Comparison of the pressure distributions over the spans of convergent bodies and bodies equivalent to them: $\delta = 10^o$ (1, 2) and 5^o (3, 4); open and filled points denote convergent and equivalent bodies respectively.

number of the incident flow $M_\infty = 4$, an angle of opening of the leading edges at the cross section of the bottom cut $\theta = 60^o$, and $\delta = 5^o$ and 10^o (curves 1). Despite the fact that the angle of inclination of the surface of the body to its symmetry plane is constant, there arises an adverse pressure gradient, i.e., an additional compression of the flow along the length of the body. Because of this, the bodies with a transverse-concave profile will be called, for short, by analogy with [3, 4], convergent bodies. For comparison, the data obtained for "equivalent" bodies with a plane downstream face are given here. In the case being considered, these bodies represent cones with a triangular cross section — so called "delta-like" wings. It is seen that the pressure along the length of the equivalent bodies is constant. Even though the pressures at the noses of the bodies of both classes are equal, the pressure at the end cross section $\bar{x} = 1$ of the convergent bodies is much higher than that of the equivalent bodies. It comprises 10.2% for the bodies with $\delta = 5^o$ and 15% for the bodies with $\delta = 10^o$, i.e., all things being equal, this pressure somewhat increases with increase in the opening angle of the initial forming cone δ_c. Calculations have shown that an adverse pressure gradient arises also at high hypersonic velocities. For example, at $M_\infty = 8$, the above-indicated increase in the pressure, as compared to the equivalent bodies, comprises 10.9% and 13.5% for the bodies with $\delta = 5^o$ and 10^o respectively.

The pressure distributions along the wing span at the end cross section $\bar{x} = 1$ of the above-considered pointed convergent bodies and bodies equivalent to them, obtained at $M_\infty = 4$, are presented in Fig. 4. This figure also shows flows around these bodies, represented in the form of equal-pressure lines (isobars). In this regime of flow around the bodies being considered, a compression shock separates from their leading edges. A cone flow with a more uniform pressure distribution along the span, which is independent of the longitudinal coordinate, is formed around the equivalent delta-like bodies. Unlike equivalent bodies, a nonstationary flow arises around the leading edges of the convergent bodies. This is explained by the fact that, even though the leading edge of these bodies is triangular in plan, it represents a spatial line with a variable slope to the longitudinal axis. It is seen from the isobar distribution presented that, in the case of convergent bodies, the front shock is located closer to the leading edge. Thus, here, there arises a less intense side flow from the downstream face to the upstream one. For this reason, a higher pressure is formed at the leading edges of the convergent bodies and the average pressure at their compression surface is much higher than that of the equivalent bodies. The above-described conditions serve to increase the total aerodynamic lift of the convergent bodies, which is ~26% larger than the lift of the equivalent bodies under the conditions being considered.

Let us determine how the above-indicated positive effect of longitudinal compression of flow can be enhanced, i.e., how the pressure at the end cross section of a body can be increased. For the above-described particular case of convergent bodies constructed on the basis of axisymmetric cones ($\delta_c = \varphi$), two additional independent parameters can be used. They are the exponent n determining the form of a body in plan and the angle of opening of the leading edges θ. The influence of the exponent n on the pressure distribution along the length of a body is demonstrated in Fig. 3. Since a decrease in $n < 1$ increases the rounding of the nose part of the body, it should be favorable for the formation of a more "two-dimensional" flow in the region of the nose. For comparison, Fig. 3 also presents some "limiting" pressure levels (lines 5 and 6) corresponding to the pressures at an axisymmetric cone and at a two-dimensional wedge with opening angles δ equal to those of the convergent bodies being considered. Moreover,

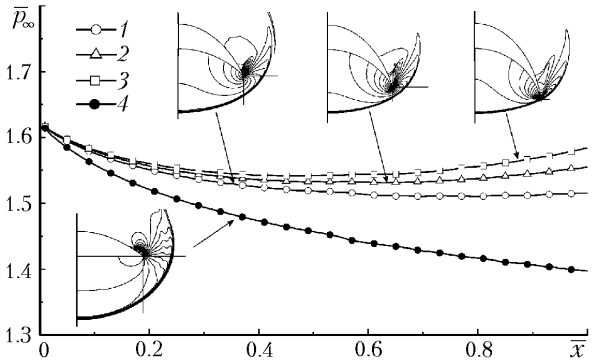

Fig. 5. Influence of the angle of opening of the leading edges θ of a body on the pressure distribution along its symmetry plane and the flow at the end cross section of the body: θ = 45 (1), 60 (2), and 75° (3); 4) equivalent body.

as a "limiting" case of the latter, so-called waveplanes can be considered. They represent three-dimensional configurations with a transverse-concave profile and a constant pressure at their surface, equal to the pressure at a wedge [13]. It is seen from Fig. 3 that the pressure at the nose of the rounded convergent bodies corresponds to the pressure at a wedge or at a waveplane even at $n \sim 0.5$, i.e., in the neighborhood of the symmetry plane of the nose there arises a two-dimensional flow. The pressure decreases immediately downstream of the nose, and then an adverse pressure gradient arises along the length of the body. As a result, the total pressure at the end cross section $\bar{x} = 1$ is higher than that of the pointed convergent bodies ($n = 1$).

Thus, a rounding of the nose part of a carrying body can increase both the pressure at the surface of the body as a whole and at its end cross section. This improves the total carrying properties of the body and increases the preliminary compression of the flow upstream of the air intake. However, it is well to bear in mind that the drag of the body increases, too, in this case. Therefore, the necessary rounding of the nose part of a flying vehicle should be selected with account for the above-indicated factors, depending on the purpose of the vehicle.

Note that, even though the rounding of the convergent bodies considered in [3, 4] increased the pressure in the neighborhood of their nose, the pressure downstream of the nose decreased fairly rapidly to the level corresponding to that of a pointed body, i.e., the rounding of the nose part of a convergent body is not effective from the standpoint of increasing the pressure at its end cross section. Unlike the indicated bodies, the bodies proposed in the present work make it possible to do this.

We also compared rounded convergent bodies with bodies equivalent to them with a plane downstream face. Figure 3 shows an example of such a comparison for an angle $\delta = 5^\circ$ at n = 0.5 and for $\delta = 10^\circ$ at n = 0.4. Even though the pressure at the nose of the rounded equivalent bodies is equal to the pressure at a wedge, the pressure in the symmetry plane downstream of their nose decreases constantly. However, the pressure at the end cross section of these bodies remains higher as compared to that of the pointed equivalent bodies (n = 1).

A flow around rounded bodies realized in the regime being considered has the following feature. In a flow around the nose part of both convergent rounded bodies and bodies equivalent to them, there arises a compression shock attaching to their leading edges. Then, downstream of these edges, e.g., at a length $\bar{x} \approx 0.15$ for a body with $\delta = 10^\circ$ and $n = 0.4$, this shock separates. The angle of inclination of the compression shock to the symmetry plane changes insignificantly along the length of the body — from the value corresponding to a two-dimensional flow around the nose to a value ~1.5–2° smaller at the end cross section. Therefore, for a nose rounded to a sufficient degree, the location of a compression shock in the symmetry plane can be predicted on the basis of the two-dimensional solution.

Another important method of increasing the pressure at the downstream face of a carrying body, in addition to the rounding of its nose part, is increasing the angle of opening of the leading edges θ at the end cross section of the body. The influence of the angle θ on the pressure in the symmetry plane of bodies based on axisymmetric cones, determined for a flow around their end cross section with $M_\infty = 4$, $\delta = 5^\circ$, $n = 0.5$, and $k = 2$, is shown in Fig. 5. At small angles θ, the pressure along the length of such a body decreases constantly; however, the effect of longitu-

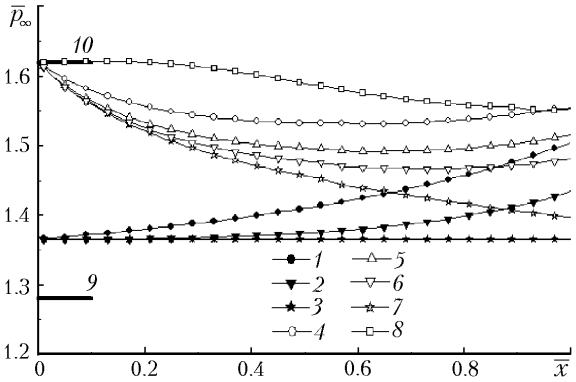

Fig. 6. Pressure distributions along the length of the symmetry plane of bodies constructed on the basis of hyperelliptic cones (filled points are pointed bodies with n = 1; open points are rounded bodies with n = 0.5): k = 2 (1, 4), 2.5 (5), 3 (2, 6); 3, 7) equivalent bodies; 8) n = 0.25, k = 3; 9) cone; 10) wedge.

dinal compression of the flow can arise with increase in θ. Calculations have shown that, in a flow around the indicated bodies realized in the regime being considered, at a length $\bar{x} \approx 0.2$ there arises a compression shock attaching to their leading edges. Then the shock separates and, as is seen from Fig. 5, the leading edges of the bodies with different values of θ are under different conditions. Since an increase in θ increases the height of a body as a whole, the distance between its leading edge and the compression shock becomes smaller and smaller. This decreases the side spreading and retains the pressure at the downstream face. In any case, this pressure is much higher than the analogous pressure of an equivalent body (curve 4).

The above-described features of the gas dynamics of flying vehicles are true for vehicles constructed on the basis of axisymmetric cones with $\delta_c = \varphi$ and k = 2. The downstream face of such bodies is arched at their end cross section; therefore, they can be easily integrated with convergent chute air intakes [2] that also have an arched leading edge. At the same time, the mathematical model proposed in the present work allows one to construct carrying bodies on the basis of more complex forming bodies — hyperelliptic cones. In this case, cross sections differing markedly from a circle can be obtained by changing the parameter k. For example, as $k \to \infty$ the cross section of such a cone tends to a square or a rectangle. Therefore, these cones can be used as a basis for construction of carrying bodies with a cross section having a much smaller curvature than the curvature of the arched cross section at $\bar{x}$ = 1. The indicated surfaces hold much promise from the standpoint of their integration with air intakes of other types, e.g., with near-planar air intakes.

The influence of the exponent k of a hyperelliptic cone on the pressure distribution along the symmetry plane of bodies constructed on its basis at $\delta_c = \varphi = 5^\circ$, $\theta = 60^\circ$, and a Mach number M_∞ = 4 is illustrated in Fig. 6. For all of the cases considered, an increase in k decreases the pressure in the symmetry plane of such a body. It should be noted that a flow around pointed bodies (n = 1) is also subjected to a longitudinal compression, even though this effect is weaker as compared to bodies constructed on the basis of axisymmetric cones (k = 2). For example, an increase in the value of k of the above-indicated bodies from 2 to 3 decreases the pressure at the end cross section by ~50%; however, this pressure is higher than the analogous pressure of the equivalent bodies with a plane downstream face. For rounded bodies with n = 0.5, the influence of the parameter k is analogous, i.e., an increase in it decreases the pressure at the end cross section. It is seen that, at $k > 3$, a flow is not compressed in the longitudinal direction. Calculations have shown that, at $k \sim 5$, the pressure in the symmetry plane of the bodies being considered is close to the corresponding pressure of the equivalent bodies. It should be noted that in a flow around the end cross section of all of the bodies being considered, realized in the regime being investigated, there arises a compression shock separating from their leading edges.

As follows from the data obtained (see Fig. 3), the above-indicated decrease in the pressure of a body can be compensated by an increase in the rounding of its nose part, i.e., by a decrease in the parameter n. Such an example is presented in Fig. 6 for k = 3 and n = 0.25 (curve 8). In this case, we obtain a body, a larger part of the wing-span surface of which has a small curvature. In a flow around this body, at $\bar{x} > 0.2$, as in a flow around the other bodies,

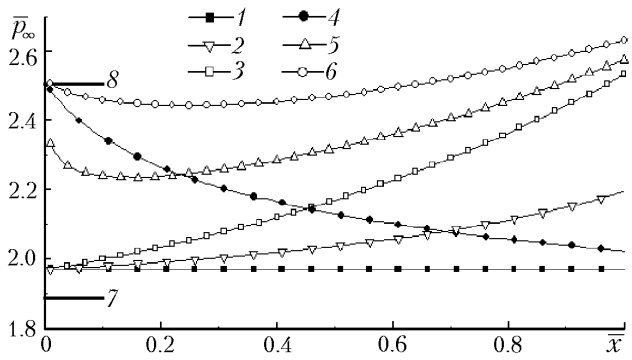

Fig. 7. Influence of the elongation λ_c of the forming hyperelliptic cones on the pressure distribution in the symmetry plane of a body: 1–3) pointed bodies; 4–6) rounded bodies; filled points are equivalent bodies; λ_c = 1 (2) and 2.02 (3, 5, 6); n = 1 (3), 0.7 (5), and 0.5 (6); 7) cone; 8) wedge.

there arises a compression shock separating from the leading edge. However, in the case of an incident flow with a large Mach number (M_∞ = 8), there arises a compression shock attaching to the leading edge along the whole of its length. In this case, at $\bar{x}$ lower than $\bar{x} \sim 0.8$, this shock is located lower than the leading-edge plane and has a convex shape; then it becomes weakly concave and is located higher than the leading edge. In the region of the rounded nose there arises a two-dimensional flow with a pressure in the symmetry plane $\bar{p}_\infty \sim 2.48$; this flow is retained constant along the whole length of the body to the end cross section. In this respect, the configuration described can be compared to a power-law waveplane [13] constructed on the basis of a two-dimensional flow downstream of an oblique compression shock and having a constant-pressure surface. However, unlike a waveplane, the pressure at a convergent body increases spanwise to the leading edge, which increases its aerodynamic lift. Under the given conditions, this superiority in lift reaches 12%.

The data presented in Fig. 6 correspond to the configurations constructed on the basis of hyperelliptic cones with a ratio between the axes λ_c = 1. The numerical calculations carried out for $\lambda_c < 1$ have shown that the longitudinal pressure gradient decreases in this case. It may be concluded that, all things being equal, a decrease in the curvature of the transverse profile weakens the effect of longitudinal compression of a flow. In this connection, we considered bodies having a transverse profile with a large curvature with the example of configurations with $\delta = 10^o$, $\varphi = 5^o$ (which corresponds to λ_c = 2.02), $\theta = 45^o$, and k = 2. The data on the pressure in the symmetry plane of these bodies, determined for a Mach number of the incident flow M_∞ = 4, are presented in Fig. 7. For pointed bodies (n = 1), the longitudinal compression of a flow significantly increases with increase in the parameter λ_c. If, at λ_c = 1 (curve 2), the increase in the pressure at the end cross section of such a body is ~11%, this increase is ~28% at λ_c = 2.02 (curve 3). In this case, the pressure at the end cross section of the body reaches values close to the pressure at a two-dimensional wedge. The total lift increased by 32% as compared to the lift of the equivalent body with a plane downstream face.

The effect of longitudinal compression of a flow also arises in configurations with a rounded nose part (curves 5 and 6); at large roundings, the pressure at the end cross section can be even higher than the pressure in the two-dimensional flow around the nose. This is due to the definite structure of the body. In particular, in a flow around the end cross section of the convergent configurations with λ_c = 2.02, which is presented in Fig. 7, there arises a compression shock attached to the leading edges. In this case, a Mach interaction is realized between the shock arising in the region of the leading edge and the shock arising in the central part of the body. The flow around the cross section of a pointed configuration with M_∞ = 4 is presented in the form of isobars in Fig. 8. In a flow around the nose part of this body, there arises a separated convex compression shock that attaches to the leading edge at $\bar{x} \approx 0.8$. As the longitudinal coordinate increases, there arises a compression shock with a deflection point and, finally, a compression shock with a Mach structure is formed near the end cross section. Note that the compression shock intersects, at the attachment point $\bar{x} > 0.8$, the leading edge; therefore, on the upstream face at the cross sections $\bar{x} \approx 0.8$ there is a trace of the shock that, up to then, was separate from the leading edge.

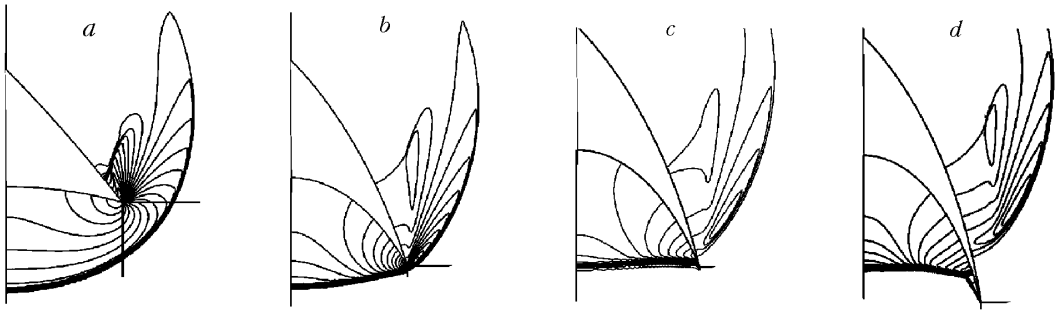

Fig. 8. Structure of the flow at the cross sections of a body ($\delta = 10^o$, $\varphi = 5^o$, $\theta = 45^o$, $n = 1$, $k = 2$): $\bar{x} = 0.2$ (a), 0.8 (b), 0.9 (c), and 1 (d).

Conclusions. The aim of the present work was to find and investigate new configurations of three-dimensional carrying bodies capable of providing higher levels of compression of a flow at their end cross section (at the site of location of the air intake of a parallel-flow, air-breathing engine used in promising flying vehicles) without an additional increase in the angle of inclination of their surface, i.e., due to only the effect of three-dimensional compression of the flow. A model for construction of such bodies is proposed. It allows one to define the form of a body in plan with the use of power functions and construct its cross section on the basis of pieces cut from the surface of a backward-facing hyperelliptic cone. This model can be used for an extended parametric analysis. The aerodynamics of the indicated bodies have been numerically investigated for the case of a supersonic flow around them. The data obtained were compared with the analogous data for "equivalent" bodies with a plane backward face. The influence of different parameters on the formation of an adverse pressure gradient along a body has been investigated. It was established that the pressure at the end cross section of a carrying body can be additionally increased by rounding of its nose part and that, in certain cases, this pressure can exceed the pressure corresponding to a two-dimensional flow.

NOTATION

a_x and b_x, major and minor semiaxes of an ellipse; $C_p = (p - p_\infty)/q_\infty$, pressure coefficient; k, exponent in the equation of a hyperellipse; L, length of a body, m; l, span of the body (its maximum transverse size), m; L_c, length of a hyperelliptic cone, m; $\bar{L}_c = L_c/L$, relative length of the hyperelliptic cone; M_∞, Mach number of the incident flow; n, exponent determining the form of the body in plan; p, pressure, N/m^2; $\bar{p} = p/p_\infty$, relative pressure; q, kinetic head, N/m^2; S_{pl}, area in plan, m^2; x, y, z, Cartesian coordinates, m; $\bar{x}$, $\bar{y}$, $\bar{z}$, relative coordinates normalized to the length of the body L; $\bar{z}_x$, relative transverse coordinate normalized to a local half-span; $\bar{z}_{pl} = z_{pl}/L$, relative transverse coordinate of the leading edge; α, angle of attack, deg; δ, angle of inclination of the surface of the body to its symmetry plane, deg; δ_c, half-angle of opening of the hyperelliptic cone in the vertical symmetry plane, deg; θ, angle of opening of the leading edges at the end cross section of the body, deg; $\lambda = l^2/S_{pl}$, elongation of the body in plane; $\lambda_c = b_x/a_x = \tan\delta_c/\tan\varphi$, elongation of the hyperellipse; φ, half-angle of opening of the hyperelliptic cone in the horizontal symmetry plane, deg. Subscripts: c, hyperelliptic cone; pl, form in plan; ∞, conditions in the incident flow.

REFERENCES

1. A. M. Blokhin, B. I. Gutov, V. V. Zatoloka, et al., Convergent input diffusers and axisymmetric supersonic conical Buseman compression flows, in: *Aerophysical Studies* [in Russian], Collection of Sci. Papers, Institute of Theoretical and Applied Mechanics of the Siberian Branch of the USSR Academy of Sciences, Novosibirsk (1972), pp. 105–108.
2. B. I. Gutov and V. V. Zatoloka, Convergent input diffusers with an initial shock wave and an additional external compression, in: *Aerophysical Studies* [in Russian], Collection of Sci. Papers, Institute of Theoretical and Applied Mechanics of the Siberian Branch of the USSR Academy of Sciences, Novosibirsk (1973), pp. 64–66.
3. Yu. P. Gun'ko, G. N. Markelov, and A. P. Shashkin, Gasdynamic designing of waveplanes with convergent compression surfaces and air intakes, *Sib. Fiz-Tekh. Zh.*, Issue 4, 47–55 (1993).

4. Yu. P. Gun'ko, I. I. Mazhul', and R. D. Rakhimov, Numerical study of a supersonic flow past a carrying body with differently shaped compression surfaces, *Teplofiz. Aéromekh.*, **7**, No. 1, 13–24 (2000).
5. Yu. P. Gun'ko, A. N. Kudryavtsev, I. I. Mazhul', R. D. Rakhimov, and A. M. Kharitonov, Gasdynamics of a convergent air intake integrated with a forebody compression surface, *Izv. Ross. Akad. Nauk*, *Mekh. Zhidk. Gaza*, No. 2, 157–169 (2001).
6. A. N. Kudryavtsev and R. D. Rakhimov, A marching procedure of numerical solution of two-dimensional and three-dimensional steady Euler equations using shock-capturing schemes, in: *Proc. Int. Conf. on the Methods of Aerophysical Research* (ICMAR-98), Pt. 1, Novosibirsk (1998), pp. 117–122.
7. Yu. P. Goonko, A. M. Kharitonov, A. N. Kudryavtsev, I. I. Mazhul, and R. D. Rakhimov, Euler simulations of the flow over a hypersonic convergent inlet integrated with a forebody compression surface, in: *Proc. Eur. Congr. on Computational Methods in Applied Science and Engineering*, Barcelona, 11–14 September 2000, CD-Rom Proceedings.
8. H. C. Yee, R. F. Warming, and A. Harten, Implicit total variation diminishing (TVD) schemes for steady-state calculations, *J. Comput. Phys.*, **57**, No. 3, 327–360 (1985).
9. B. Einfeldt B., C. D. Munz, P. L. Roe, and B. Sjogreen, On Godunov-type methods near low densities, *J. Comput. Phys.*, **92**, No. 2, 273–295 (1991).
10. W. K. Anderson, J. L. Thomas, and B. van Leer, Comparison of finite volume flux vector splitting for the Euler equations, *AIAA J.*, **24**, No. 9, 1453–1460 (1986).
11. L. C. Squire, Pressure distributions and flow patterns at M = 4 on some delta wings, *Aeronaut. Res. Council*, *Reports and Memoranda*, No. 3373 (1964).
12. Yu. P. Gun'ko and I. I. Mazhul', Flow past the lower surface of V-shaped wings under the off-design operating conditions at Mach numbers smaller than the calculated one, *Izv. SO AN SSSR*, *Ser. Tekh. Nauk*, No. 3, Issue 1, 8–12 (1977).
13. I. I. Mazhul' and R. D. Rakhimov, Numerical study of off-design conditions of flow past power-law wave-planes based on flows with plane compression shocks, *Izv. Ross. Akad. Nauk*, *Mekh. Zhidk. Gaza*, No. 5, 168–177 (2003).